Supplementary Materials for

Study on fabricating transparent, stretchable, and self-healing ionic conductive elastomers from biomass molecules through solvent-free synthesis

Zhaolin Wu, Yuhang Guo, MingZhi Qin, Chaoyou Liao, Xiufen Wang*, and Liqun Zhang*

*Corresponding author. Email:

wangxf1@mail.buct.edu.cn; zhanglq@mail.buct.edu.cn

Zhaolin Wu, Yuhang Guo, MingZhi Qin, Chaoyou Liao, and Prof. Dr. Xiufen Wang*

Beijing Engineering Research Center of Advanced Elastomers, Beijing University of Chemical Technology, 100029 Beijing, People's Republic of China

State Key Laboratory of Chemical Resource Engineering, Beijing University of Chemical Technology, 100029 Beijing, People's Republic of China

Prof. Dr. Liqun Zhang*

Beijing Engineering Research Center of Advanced Elastomers, Beijing University of Chemical Technology, 100029 Beijing, People's Republic of China

State Key Laboratory of Organic-Inorganic Composites, Beijing University of Chemical Technology, 100029 Beijing, People's Republic of China

The supporting information includes:

Materials, Materials synthesis, General characterization, and other tests.

Fig. S1, S2, & S3 ^{1}H-NMR spectra of TA and TA-co-HA.

Fig. S4 Raman characterization.

Fig. S5 & S6 FT-IR spectra characterization.

Fig. S7 & S8 DSC characterization.

Fig. S9 TG characterization.

Fig. S10 Digital photos of copolymers based on different acrylate monomers.

Fig. S11 EDS spectra of THICE.

Fig. S12 Typical Nyquist impedance spectra of THICEs.

Fig. S13 State of HA homopolymer and copolymer.

Fig. S14 Ionic conductivities of the HA homopolymer and copolymers.

Fig. S15 & Table S1 Conductivity profile as a function of temperature for THICE.

Fig. S16 Electrical performance of THICE-LiTFSI.

Fig. S17 Digital photos of THICE-LiTFSI.

Fig. S18 Cross-sectional SEM images.

Fig. S19 & S20 Decomposition of THICE and the hydrogel.

Fig. S21 Changes of ion conductivities within 7 days.

Fig. S22 Stability of THICE and hydrogel within 90 days.

Fig. S23 Flame retardant of THICE.

Fig. S24 Mechanical Properties of THICE (75 mol% HA).

Fig. S25 & S26 Mechanical properties and toughness of PTA-co-HA.

Fig. S27 Strain–stress curves with different strain rates of THICE.

Fig. S28 & S29 Photos of the self-healing experiment of THICE.

Table S2 The mechanical properties and conductivity of recycled THICE.

Fig. S30 & S31 Digital photos of the THICE immersed in solution.

Fig. S32 & S33 Recycled process of TA and characterization of recycled TA.

Table S3 The comparison between this work and prior publish results.

1.1 Materials

All the chemicals were applied as received without further purification. Thioctic acid (TA, 99%), 2-hydroxyethyl acrylate (HA, 99%), Ethyl Acrylate, Butyl Acrylate, 4-Hydroxybutylacrylate, Lithium chloride (LiCl, AR), LiTFSI were purchased from Shanghai Macklin, China. Aluminum chloride ($AlCl_3$, AR) and sodium hydroxide (NaOH, AR) were purchased from Fu-Chen Chemical Corporation, China.

1.2 Materials synthesis

The thioctic acid ionic conductive elastomer was prepared by the rapid one-pot method. The typical synthesis procedure was as follows. Lithium chloride (0.2 g) was first dissolved in hydroxyethyl acrylate (3 g) by ultrasound. Thioctic acid (6 g) and aluminum chloride ($AlCl_3 \cdot 6H_2O$, 0.07 g) were heated to 140 °C with string for 15 min until the aluminum ions are completely dissolved. Then the HA/LiCl was slowly added to the above system and stirred for 1 min. The obtained liquid was poured into a mold and kept at room temperature for cooling and named THICE [with a molar ratio of TA:HA:Li:Al(III) = 100:90:16:1]. The performance of THICE was adjusted by changing the content of aluminum chloride, lithium chloride, and acrylate. Other elastomers were prepared by a similar method.

The hydrogels for comparison were prepared by the resembling methods in the literature. Typical synthesis steps were as follows. The Acrylamide (4 g, 0.06 mol) and LiCl (1.7 g, 0.04 mol), crosslinking agent (0.1 mol%), and initiator (1 mol%) were dissolved in the 20 ml water consecutively. Polyethylene glycol diacrylate (PEGDA) was used as the crosslinker, and ammonium persulfate was used as the initiator. The solution was then transferred into a

PTFE mold and heated in an oven at 50 °C for 2 h to obtain the hydrogel.

2.1 General characterization

FT-IR spectra were recorded on a Bruker Tensor II FT-IR spectrometer with ATR mode. The transparency tests were performed on a UV-Vis spectrophotometer (Shimadzu UV-3600plus). The THICEs were heated and attached to quartz slices as the test samples for the UV–vis spectra, the thickness of the THICE film used in the UV spectrum test was about 1 mm. The wavelength for testing was set from 1000 to 300 nm. The thermal stability was recorded by a TA instrument Q50 at a heating rate of 20°C min^{-1} (40 to 550°C). The other thermal properties were measured by differential scanning calorimetry at a heating rate of 10°C min^{-1} (TA instrument Q100). Both instruments used nitrogen as the purge gas. The stress relaxation characteristics were performed on rectangular specimens (ca. 1 mm (T) × 6 mm (W) × 50 mm (L)) by TA-Q800 DMA apparatus at room temperature. The characteristic relaxation time (τ) was calculated by **Equation S1**.

$$\sigma(t) = \sigma_e + \left(\sigma_0 - \sigma_e\right) e^{-\frac{t}{\tau}}$$

$$(S1)$$

2.2 Mechanical characterizations

Mechanical properties were tested by a CMT4104 instrument at a fixed stretching rate of 50 mm min^{-1} at room temperature. The tensile strength and elongation at break measurements were based on more than 5 samples. Dissipated energy and hysteresis ratios in the loading-unloading tests were calculated by **Equations S2** and **S3** respectively.

$$E_{Dissipated} = \int \sigma d\varepsilon_{loading} - \int \sigma d\varepsilon_{unloading}$$

$$(S2)$$

$$Hysteresis\ ratio = \frac{\int \sigma d\varepsilon_{loading} - \int \sigma d\varepsilon_{unloading}}{\int \sigma d\varepsilon_{loading}} \times 100\% \tag{S3}$$

2.3 Ionic conductivity test and electrical characterizations

Electrochemical impedance spectroscopy (EIS) tests were performed on an electrochemical workstation (CHI660E). All conductivity tests were replicated with at least 3 samples.

The samples were fixed between two steel round electrodes and the ionic conductivity was calculated by **Equation S4**, where σ is the ionic conductivity, L is the effective length, S is the cross-sectional area, and Z' is the real part of the impedance.

$$\sigma = \frac{L}{RS} = \frac{L}{Z'S} \tag{S4}$$

The Vogel–Tamman–Fulcher (VTF) equation was used to describe non-Arrhenius dependence on temperature and the ionic conductivity (**Equation S5**), where σ_∞ is the limiting value of the ionic conductivity depending on the number of charge carriers, E_a is equivalent to the activation energy for ion motion, D is the strength parameter, T is the temperature and T_0 is Vogel temperature (usually $T_0 = T_g - 50$ K).

$$\sigma_{(T)} = \sigma_\infty e^{-\frac{E_a}{R(T-T_0)}} = \sigma_\infty e^{-\frac{D}{T-T_0}} \tag{S5}$$

The decomposition voltage of ICE and hydrogel electrolyte were tested via linear sweep voltammetry (LSV), and the scan rate was set at 0.1 mV s^{-1} in the range from 0 to 10 V.

The THICEs were cut into a series of rectangular samples. Two copper wires were attached to both ends of the ICE for testing. The relative resistance changes with the applied strain were recorded by the DMM7510 Digital Graphical Sampling Multimeter (Keithley Instruments, USA). The variation of the relative resistance was calculated by **Equation S6**.

The Gauge Factors (GF) were obtained by **Equation S7**.

$$\frac{\Delta R}{R_0} = \frac{R - R_0}{R_0} \times 100\%$$

(S6)

$$GF = \frac{\Delta R / R_0}{\varepsilon}$$

(S7)

Theoretically, the relative resistance and elongation should meet the quadratic function relationship. When the resistive sensor of ICE is stretched by a factor of λ (λ = 1+ε), the volume resistance can be described by **Equations S8** and **S9**.

$$R = \frac{L}{\sigma S} = \frac{L_0 \lambda}{\sigma {S_0}/{\lambda}} = \frac{L_0}{\sigma S_0}\lambda^2 = R_0 \lambda^2 = R_0 \left(1 + \varepsilon\right)^2$$

(S8)

$$\frac{R - R_0}{R_0} = (1 + \varepsilon)^2 - 1$$

(S9)

The wearable sensors for detecting the joint motions were tested by the similar methods.

2.4 Recycling and self-healing characterizations

Self-healing tests were conducted by cutting the specimens into two parts and healing them at room temperature for a different duration. Negligible pressure (<0.1 N) was exerted for a short period (<10 s) to guarantee a greater touch of the clipping planes. Recycling specimens were obtained by the fractured THICE re-heated at 140 °C for 15 min, then cooled to room temperature. The self-healing efficiencies were calculated by **Equation S10**, where $\varepsilon_{b,0}$ is the elongation at the break of the original specimen and ε_b is the elongation at the break of the newly obtained specimen.

$$\eta = \frac{\varepsilon_b}{\varepsilon_{b,0}} \times 100\%$$

(S10)

3 Supporting Figures
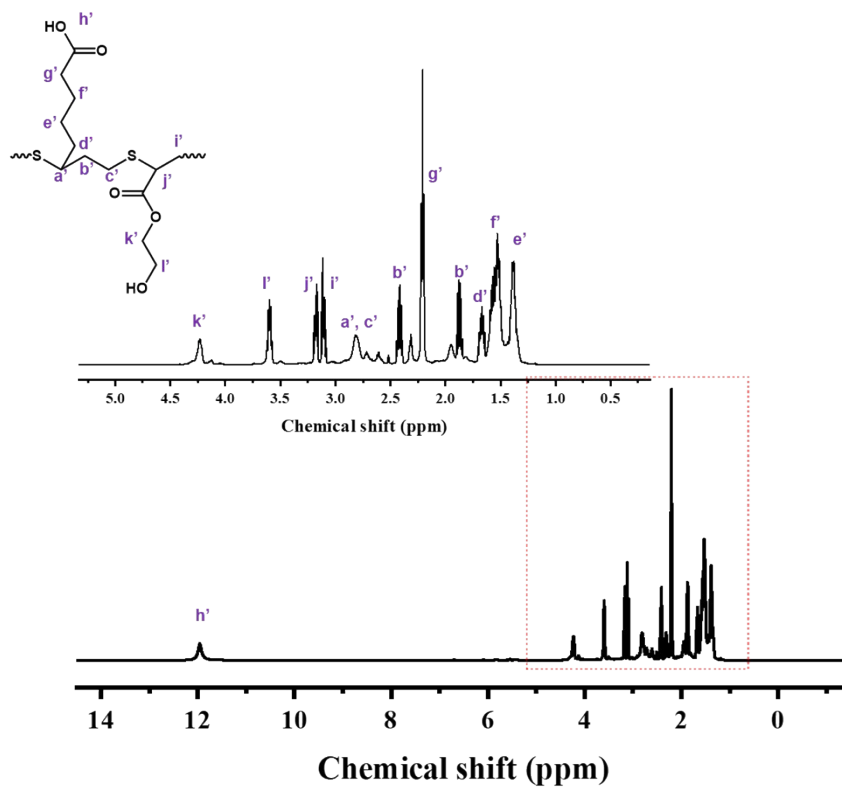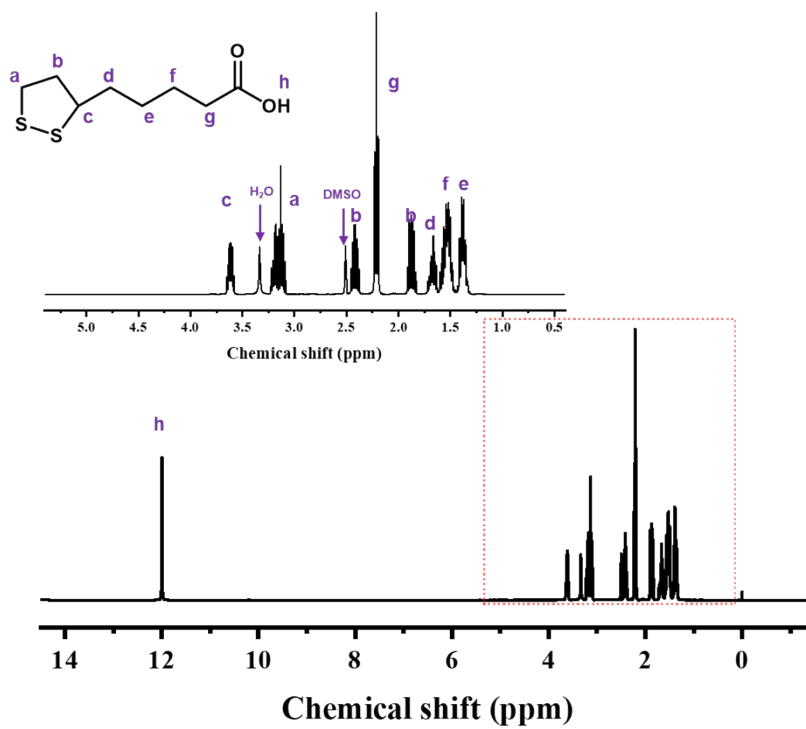
Figure S1 ^{1}H-NMR spectrum of TA.

Figure S2 ^{1}H-NMR spectrum of TA-co-HA.

As shown in Figures S1 and S2, the proton peaks (a, c) for TA were located at 3.13 ppm, and

3.61 ppm, respectively. After copolymerization, the chemical shifts of these two proton peaks

(a'/c' at 2.80 ppm) were changed, indicating the occurrence of ring-open polymerization. The

presence of new proton peaks (j' at 3.16 ppm, i' at 3.09 ppm, l' at 3.59 ppm, k' at 4.23 ppm)

showed that the alkene double bonds of HA successfully quenched the radical chain ends by

inverse vulcanization [42,43,55,56].
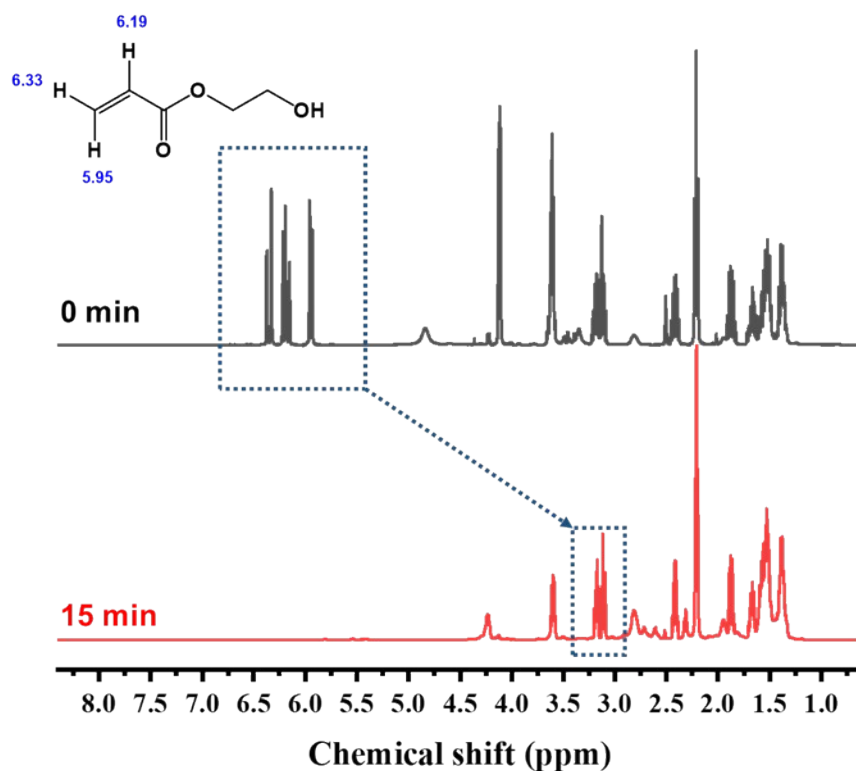
Figure S3 ^{1}H-NMR spectra determined at 0 and 15 minutes for the TA-co-HA thermal polymerization. The changes in the chemical shifts of the vinyl protons confirmed the successful reaction between TA and HA. Additionally, there was no chemical shift of double bonds in HA from 5 ppm to 7 ppm, indicating there were no residual HA monomers.
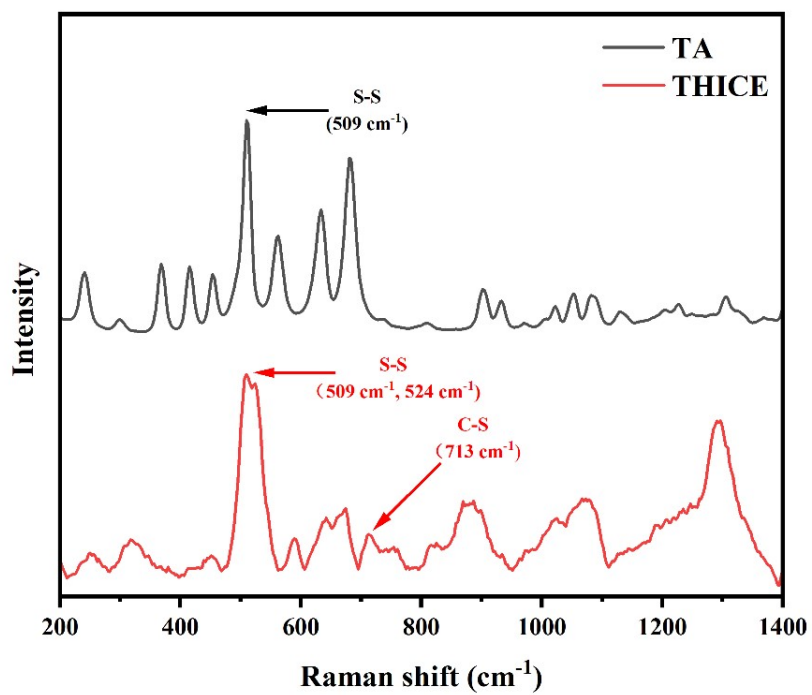
Figure S4 Raman spectra of TA powder (black line) and THICE (red line).
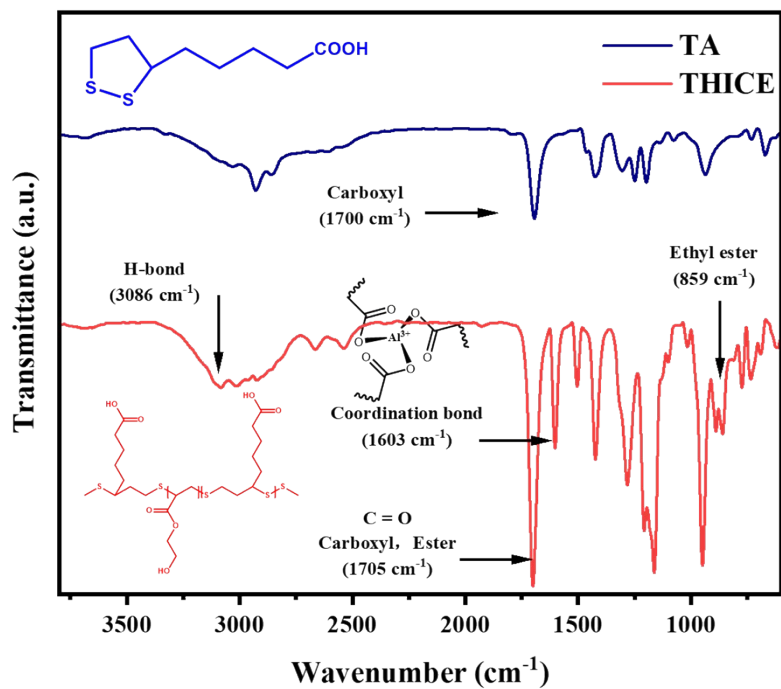
Figure S5 FT-IR spectra of TA powder (blue line) and THICE (red line).
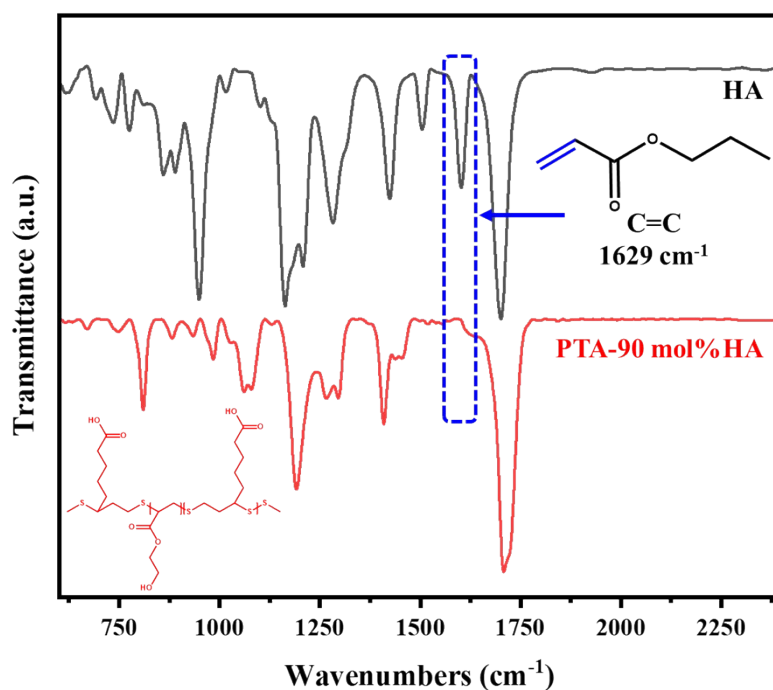
Figure S6 FT-IR spectra of the HA monomer (black line) and TA-HA copolymers (red

line).
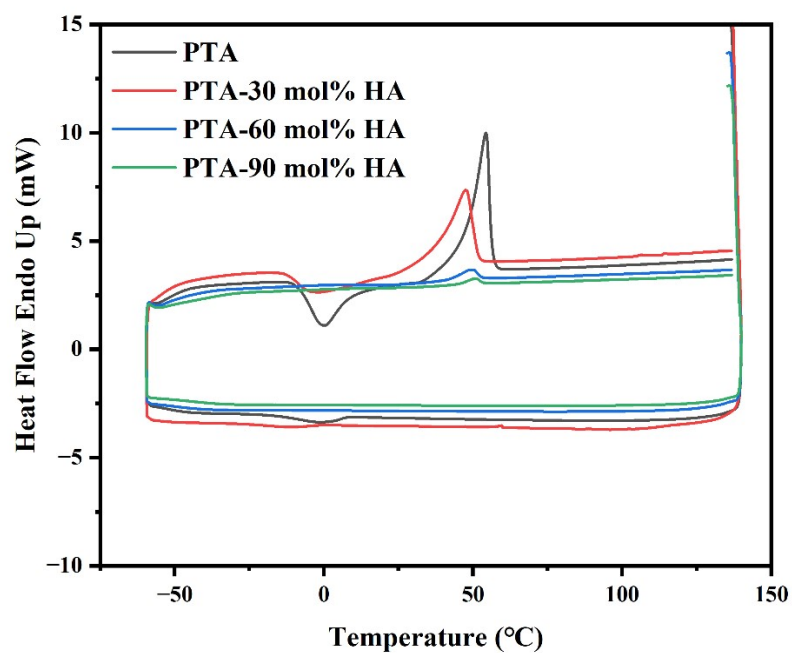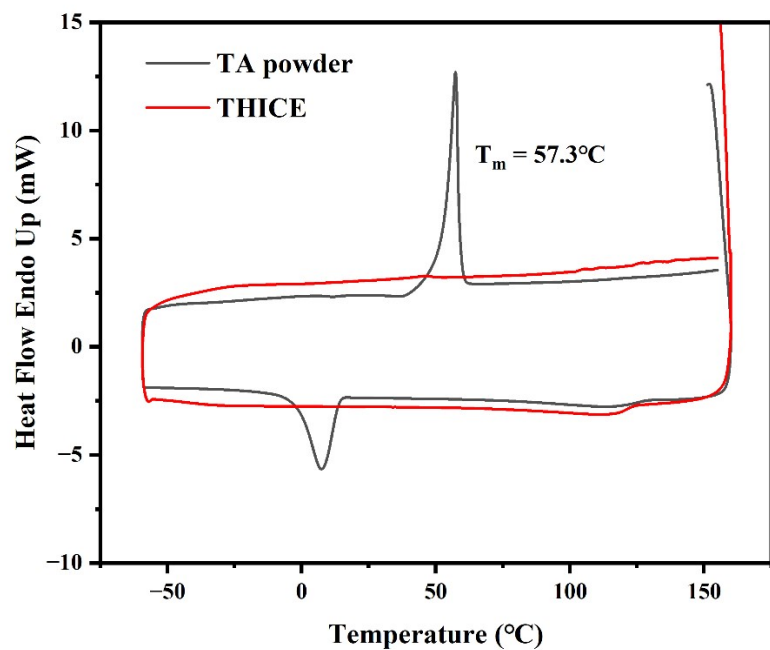
Figure S7 DSC curves of TA (black line) and THICE (red line).

Figure S8 DSC curves of TA-HA copolymers. The TA monomer crystallization peak gradually decreased with increasing HA ratios, which indicated that HA prevented the

depolymerization of copolymer and THICE.
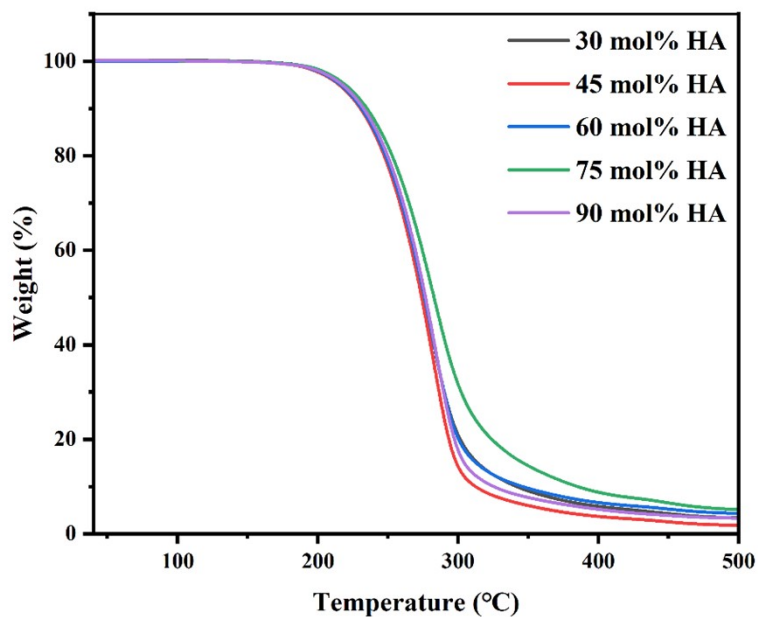
Figure S9 TG curves of THICE. This result shows that there was no residue of the HA. The
initial decomposition temperatures ($T_{5\%}$) of THICE were between 215℃ and 219 ℃, and
there was almost no mass loss of THICE below 200℃.
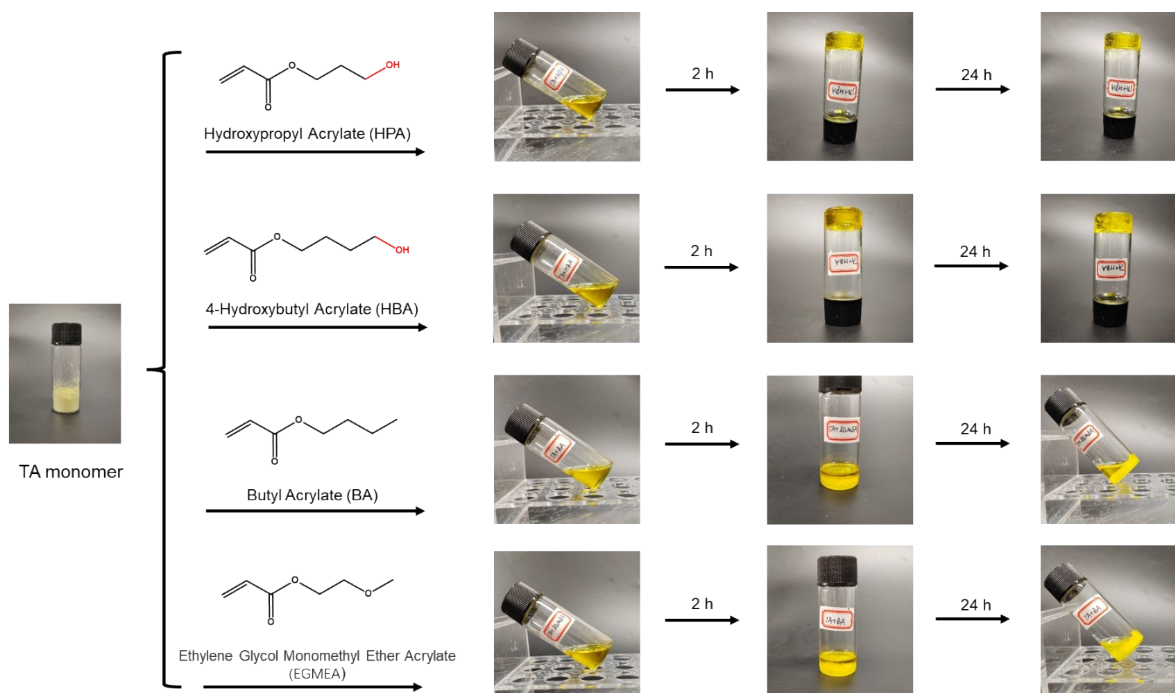
Figure S10 Thermal polymerizations of TA and acrylate. The acrylic ester in the figure included hydroxypropyl acrylate (HPA), 4-hydroxybutyl acrylate (HBA), butyl acrylate (BA), and 2-mehtoxyethyl acrylate (ethylene glycol monomethyl ether acrylate, EGMEA). The molar ratio of TA: acrylic ester was 100: 90. TA and acrylic ester were heated to melt, forming a transparent yellow solution. After 2 h, TA-HPA and TA-HBA formed transparent polymers, respectively. However, TA was precipitated out due to depolymerization in the TA-BA and TA-EGMEA systems. This result indicated that TA tends to polymerize with vinyl monomers with hydroxyl groups.
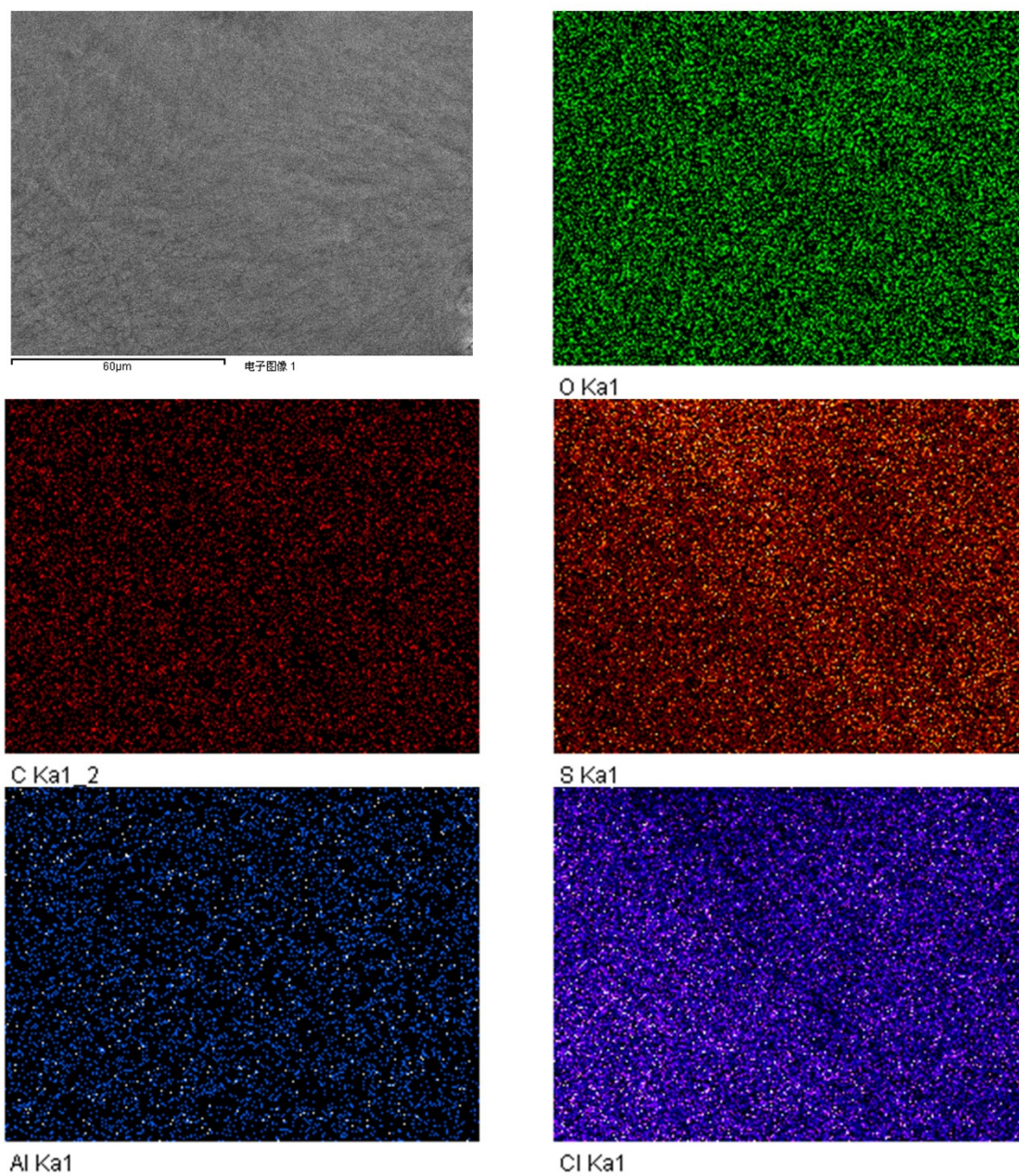
Figure S11 Energy-dispersive spectroscopy spectra of THICE. The EDS map indicated that C, O, S, Al, and Cl were uniformly distributed in the bulk THICE. This result showed that $AlCl_3$ and LiCl were homogeneously distributed in the THICE.
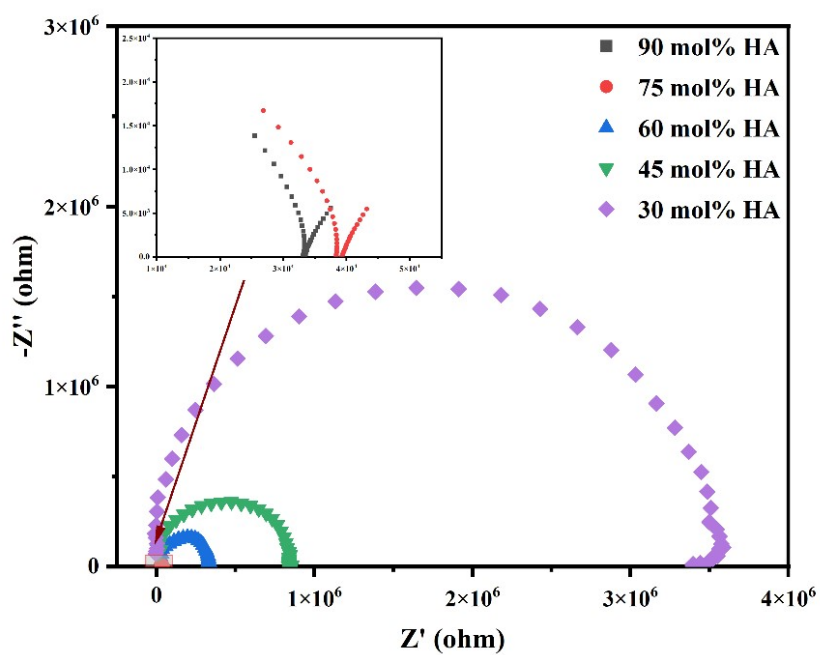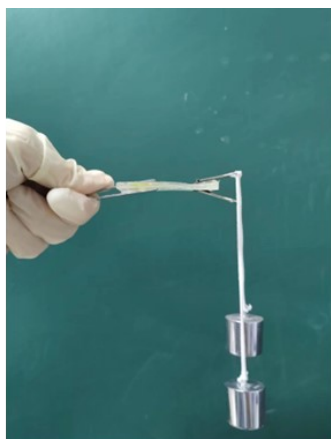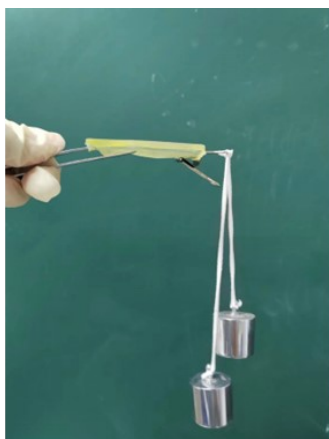
Figure S12 Typical Nyquist impedance spectra of THICEs under different HA compositions.

The impedance of THICE decreases with the increasing HA ratio.

HA homopolymer　　**AA-HA copolymer**　　**BA-HA copolymer**

Figure S13 State of HA homopolymer and copolymer. HA homopolymer, HA, and AA copolymer (with a molar ratio of AA:HA:LiCl = 100:90:16), HA and BA copolymer (with a molar ratio of BA:HA:LiCl = 100:90:16) were prepared separately. The HA homopolymer and HA-AA copolymer are rigid transparent plastics, while the BA-HA copolymer is an opaque elastomer.
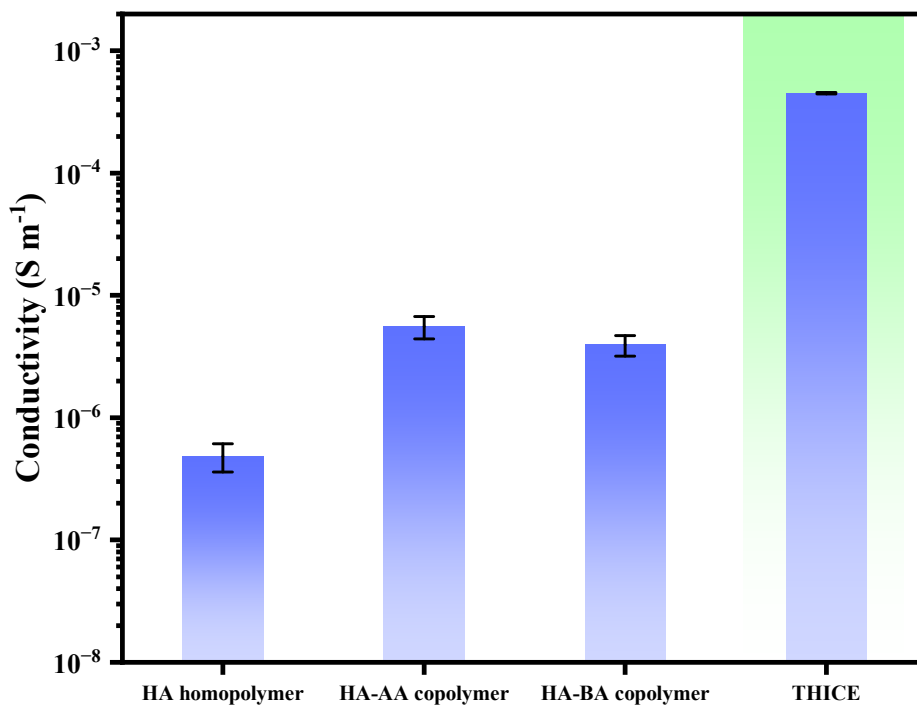
Figure S14 Ionic conductivities of HA homopolymer and copolymers.

The HA homopolymer had the lowest conductivity of the four samples. The HA monomer solvates lithium salts effectively, but the conductivities of HA homopolymers are low due to the high densities of hydrogen bonds. The flexibilities of the networks were increased by copolymerization, thus improving the conductivities of the copolymers.
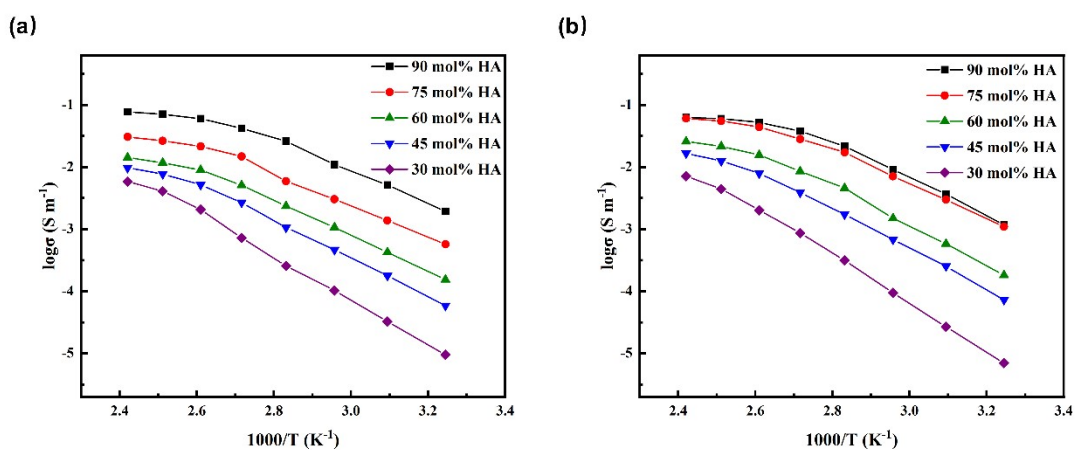
Figure S15 Conductivity profile as a function of temperature for THICE, and the contents of LiCl are (a) 8 mol% and (b) 16 mol%, respectively.

Table S1 Fitting parameters of THICE of the VTF equation.

	HA (mol%)	T_0 (K)	D	σ_∞ (S m^{-1})	E_a (J mol^{-1})	R^2
	90	275.5	0.265	0.539	606.6	0.97
	75	268.1	0.380	0.417	847.5	0.95
8 mol% LiCl	60	269.7	0.403	0.305	902.6	0.96
	45	265.5	0.524	0.302	1155.7	0.96
	30	258.6	0.809	0.334	1739.1	0.95
	90	281.4	0.221	0.063	516.4	0.96
	75	274.9	0.294	0.068	672.8	0.96
16 mol% LiCl	60	269.0	0.453	0.059	1013.5	0.97
	45	266.5	0.530	0.051	1173.7	0.96
	30	259.8	0.837	0.052	1808.3	0.96

The conductivity maximum (σ_∞) is the result of a competition between ion concentration and mobility. The σ_∞ varied from approximately 0.30 S·m^{-1} to 0.54 S·m^{-1} for all THICE with 8 mol% LiCl, while the σ_∞ varied from about 0.05 S·m^{-1} to 0.07 S·m^{-1} for all THICE with 16 mol% LiCl. This result indicated that the migration of lithium ions was inhibited at high concentrations.
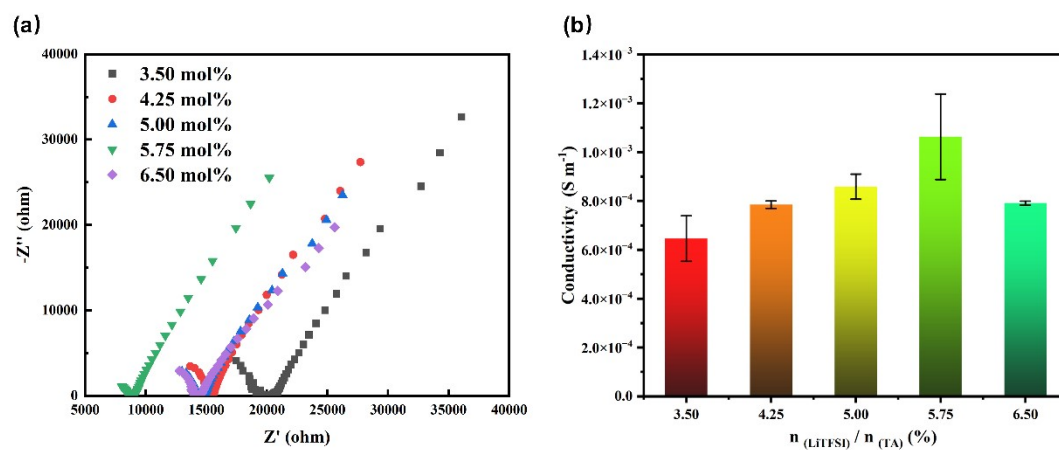
Figure S16 (a) Nyquist plots of the impedance spectra; (b) ionic conductivities of THICE-

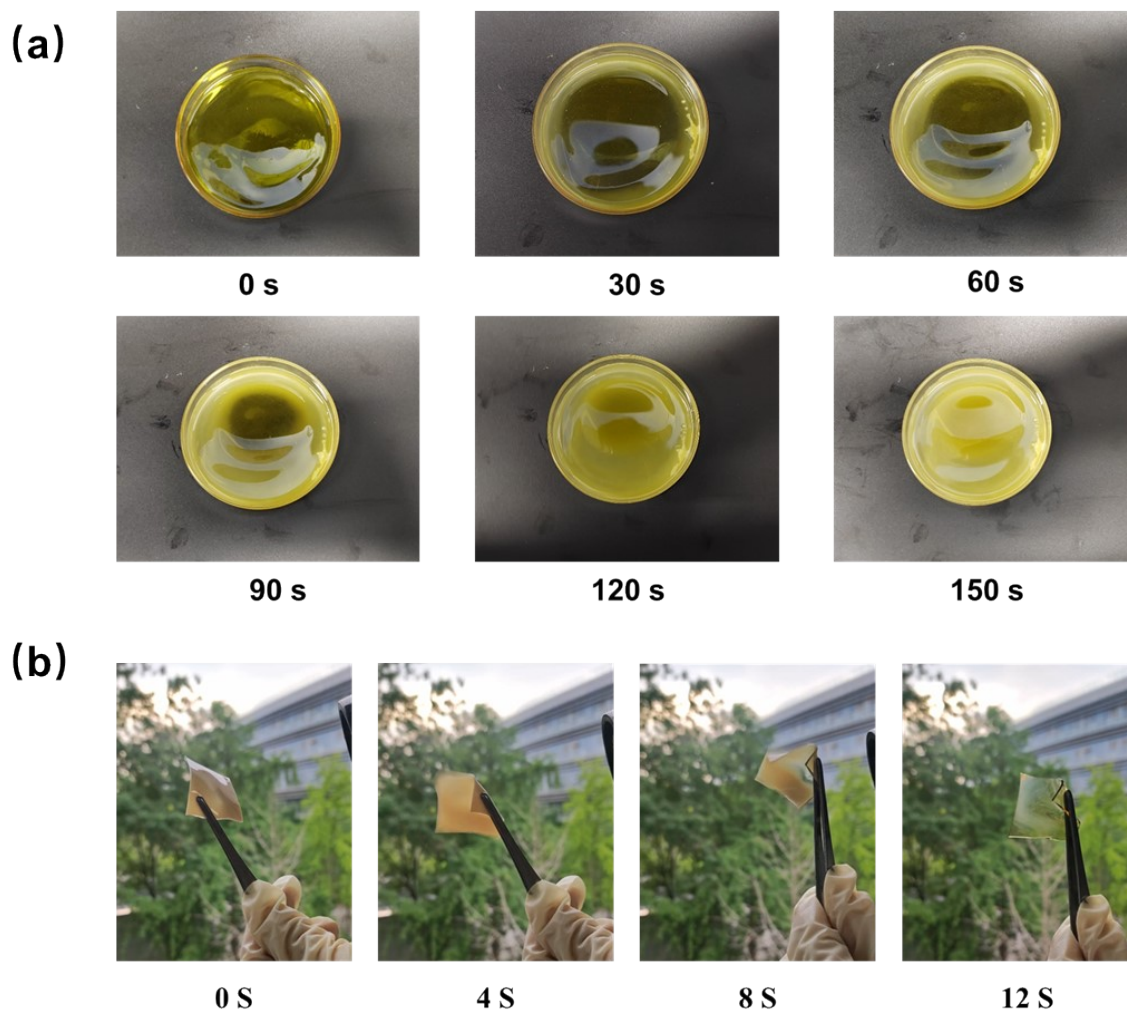LiTFSI. (The LiTFSI ratio is n (LiTFSI)/n (TA).)

Figure S17 Digital photos of THICE-LiTFSI. (a) The transition from transparency to opacity of THICE-LiTFSI during cooling; (b) the transition from opacity to transparency in THICE-LiTFSI by heating.

The transparency and opacity of THICE were reversible, which indicated that the transformation was a physical change rather than a chemical reaction. On the one hand, when THICE-LiTFSI melts, it was transparent but it gradually became opaque during the cooling process. On the other hand, when THICE-LiTFSI was heated with hot air for approximately 10 seconds, the THICE became transparent again.
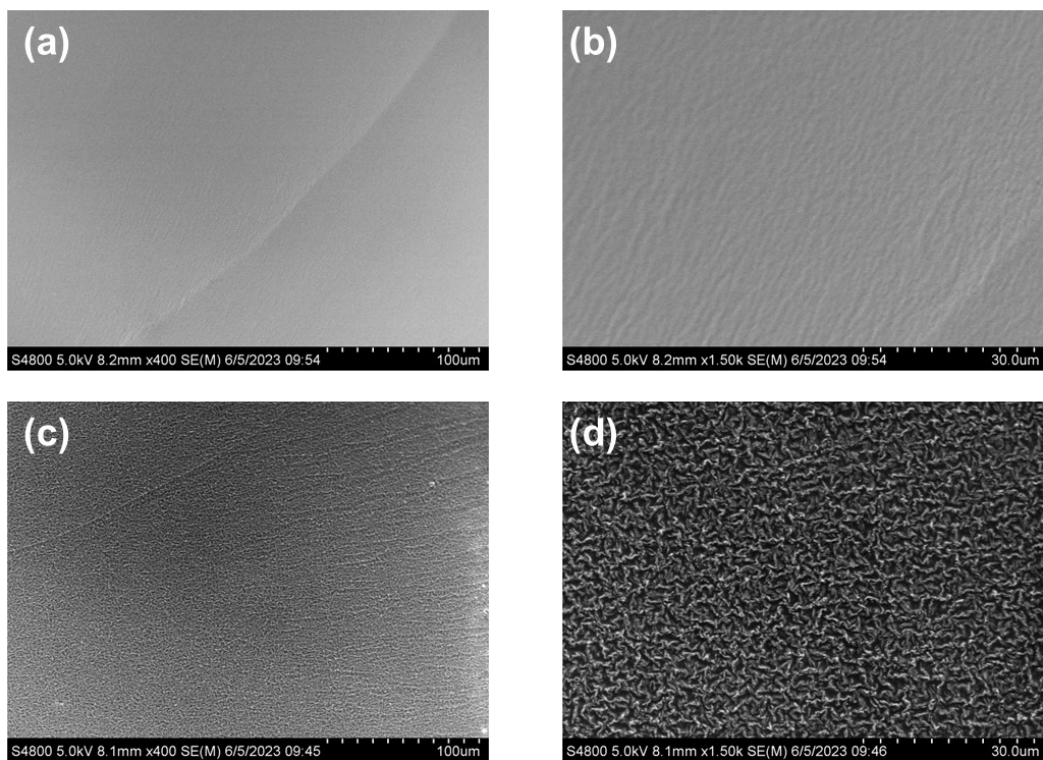
Figure S18 Cross-sectional SEM images of (a) TA-co-HA (×400), (b) TA-co-HA (×1500),

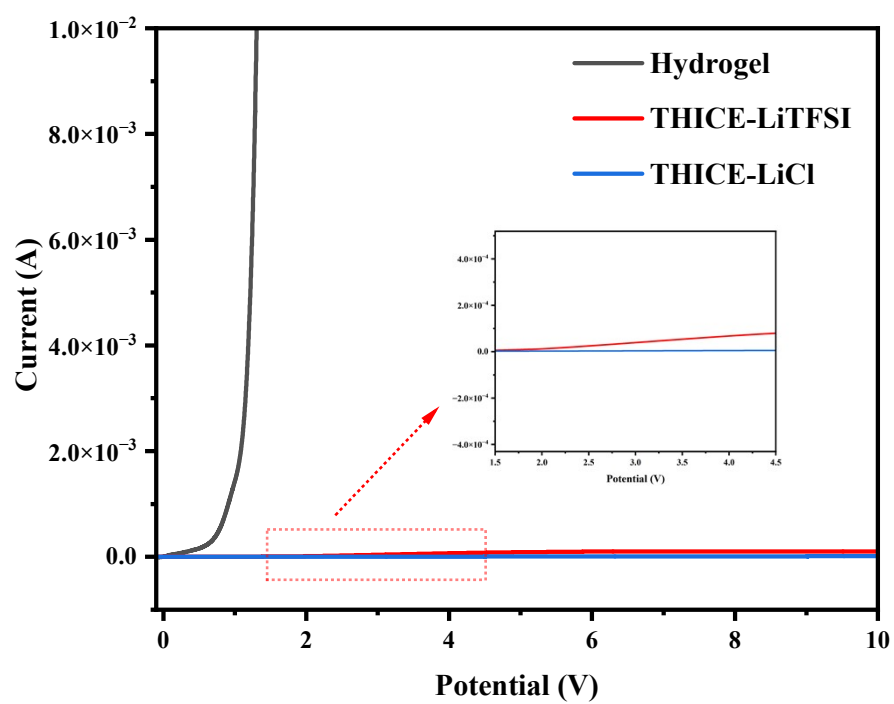(c) THICE-LiTFSI (×400), and (d) THICE-LiTFSI (×1500).

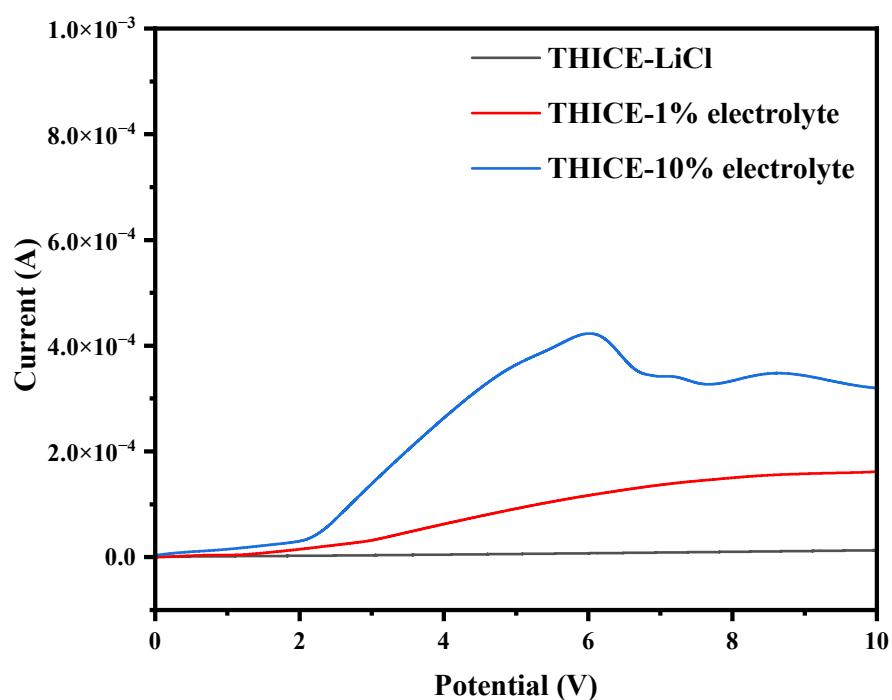**Figure S19** Decomposition voltage testing of THICE and the hydrogel.

Figure S20 Decomposition voltage testing of THICE and its organic gels. LSV scans were used to demonstrate the absence of residual HA monomer in THICE. To show the effects of small molecule residues on the decomposition voltage, 1% and 10% of the electrolyte (tetra-ethylene glycol dimethyl ether, with the molar ratio of TA: electrolyte) were added to the THICE. Here, the electrolyte did not participate in the polymerization and was present as a liquid in THICE. As shown in Fig. C4, the decomposition voltages of these THICEs decreased sharply, indicating the reduced electrochemical stability. Even with only 1% electrolyte, the electrochemical stability of THICE also declined significantly.
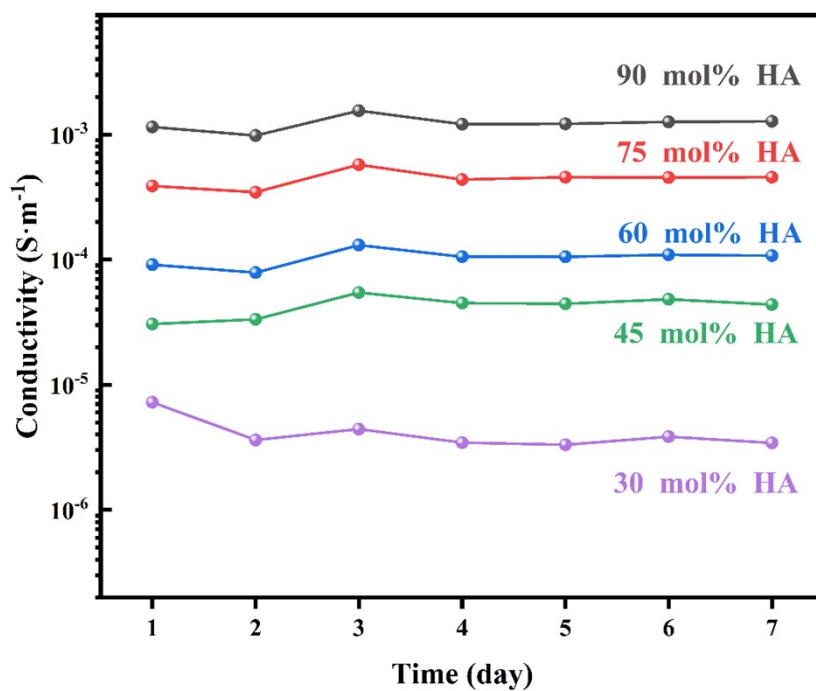
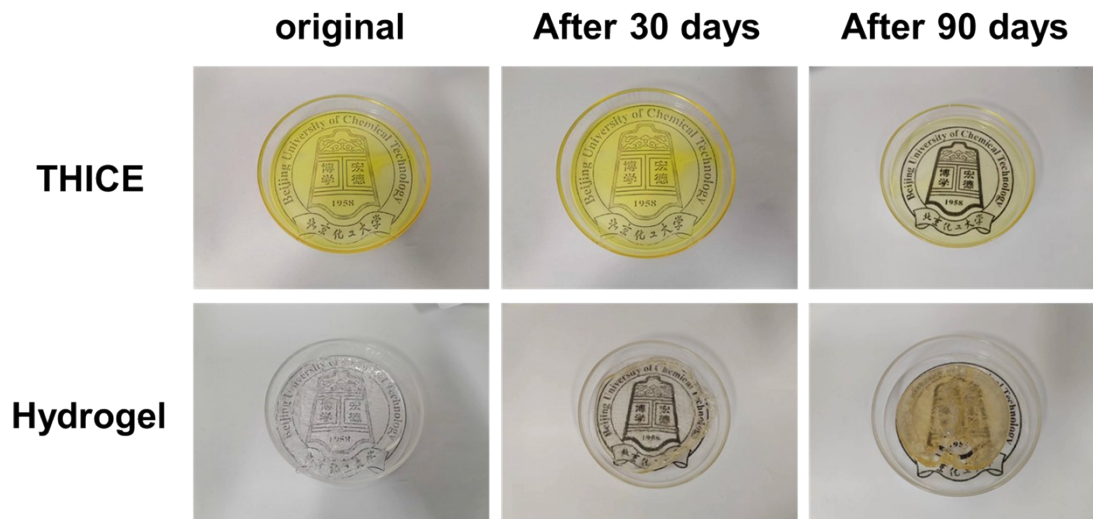**Figure S21** Changes of ion conductivities within 7 days.

Figure S22 State changes of THICE and hydrogel within 90 days at room temperature and in an atmospheric environment. There was no change in the size or the transparency for THICE after 90 days, while the size of the hydrogel reduced significantly and became non-transparent.
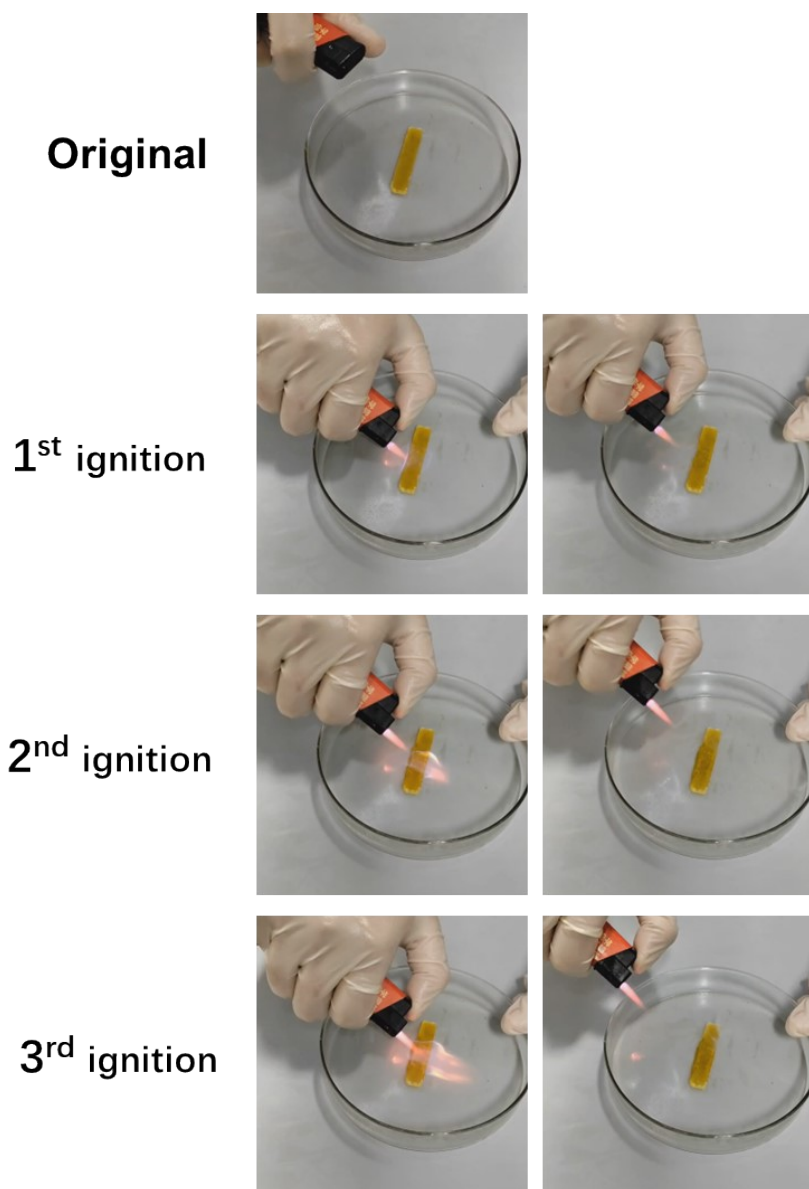
Figure S23 Flame retardant of THICE. Photo images of flammability test on the THICE. THICE is self-extinguishing, which may be attributed to its all-solid characteristics and the ability to capture free radicals for TA.
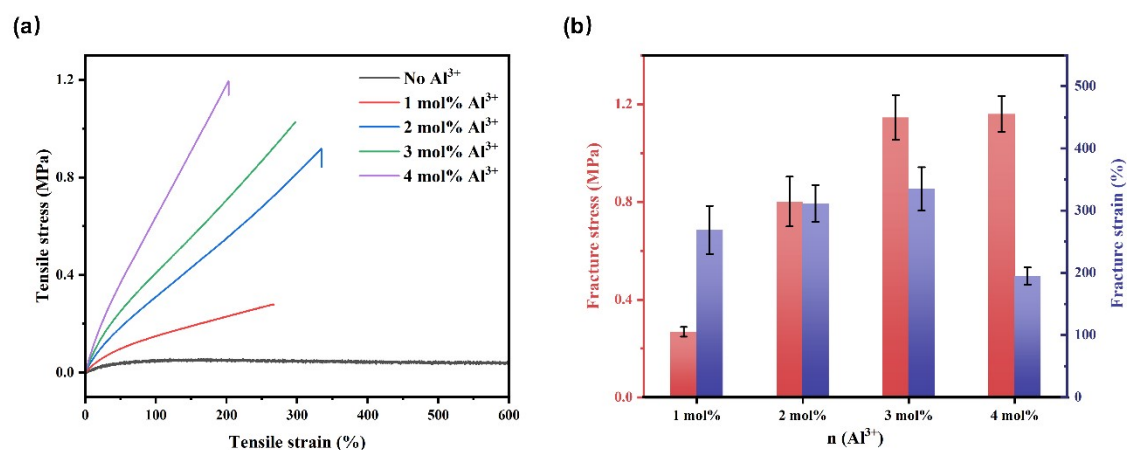
Figure S24 (a) Mechanical Properties of THICE (75 mol% HA); (b) fracture strength and elongation values with different Al (III) ion content.
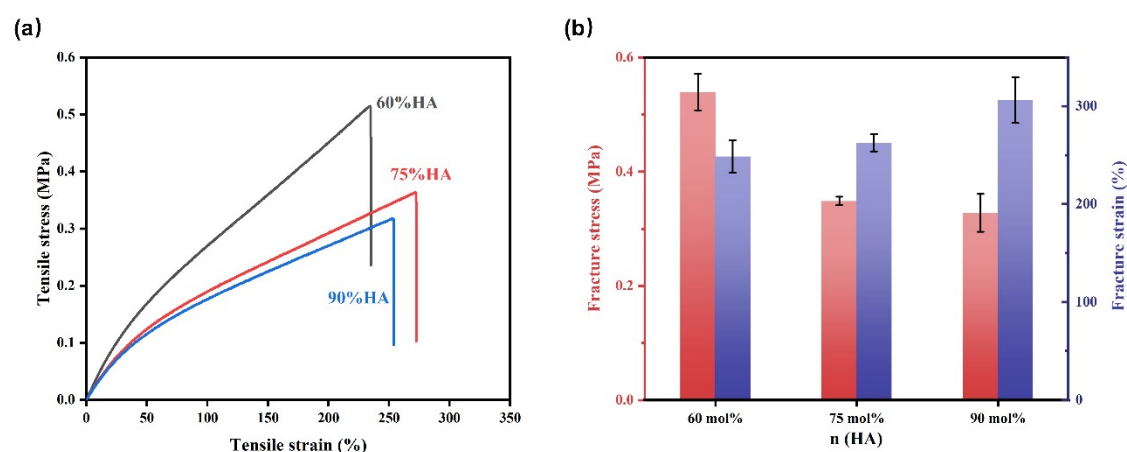

Figure S25 (a) Mechanical Properties of PTA-co-HA without LiCl; (b) fracture strength and elongation values with different HA content.

With the increase in the proportion of HA, the tensile strength of PTA-co-HA decreased and the elongation at break increased. When the proportion of HA was low (<60 mol%), the material was brittle and had difficulty with stripping.
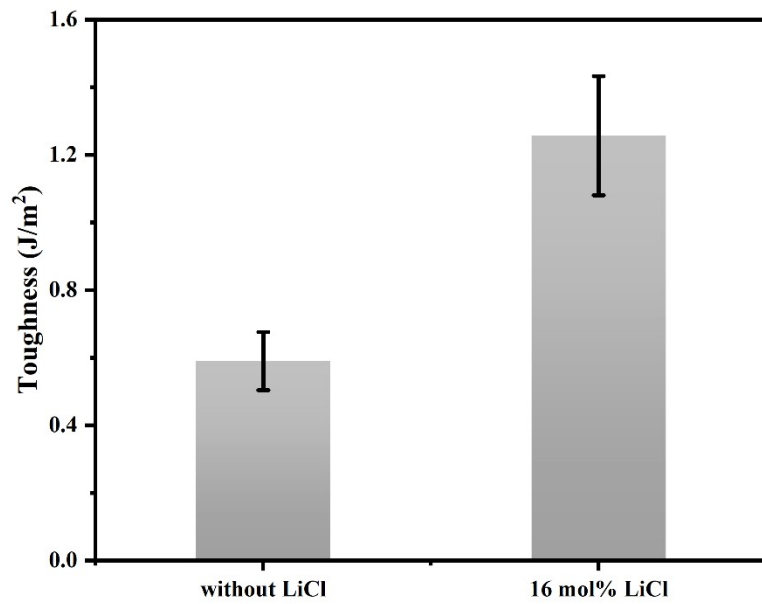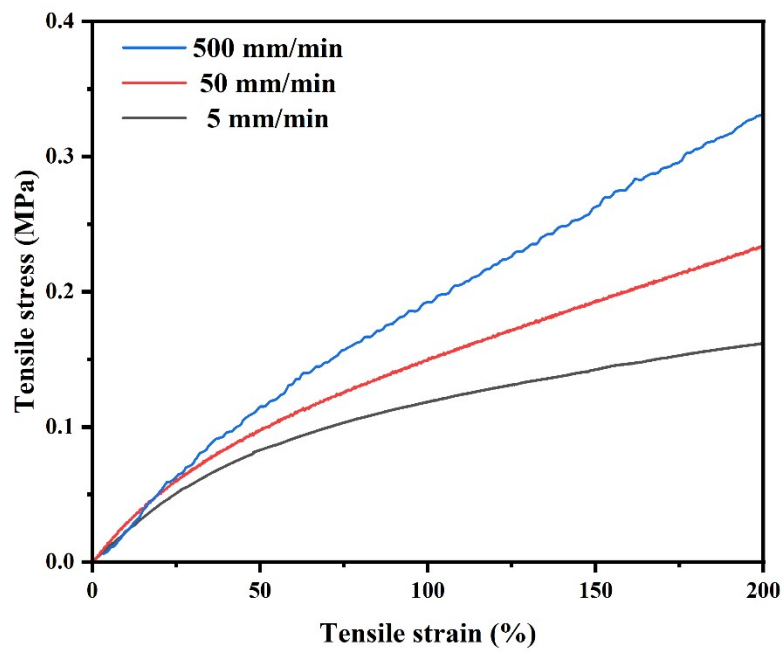
Figure S26 Toughness of PTA-co-HA and THICE [both with molar ratios of TA:HA:Al(III)

= 100:90:1].

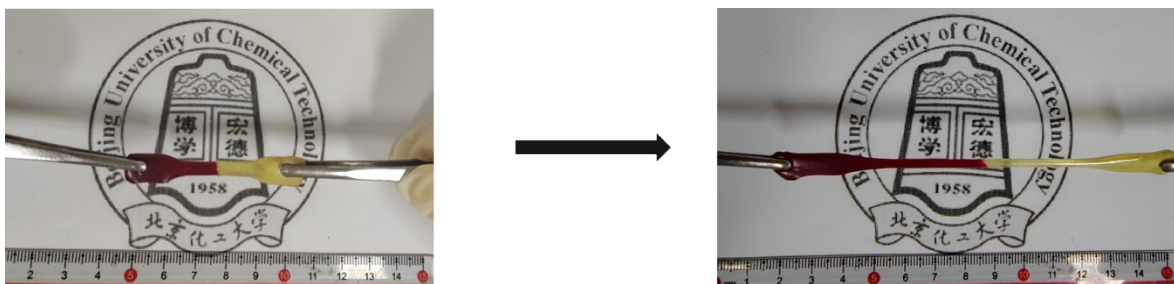**Figure S27** Strain–stress curves with different strain rates of THICEs.

Figure S28 Photos of the self-healing experiment of THICE. The Photo shows that THICE was cut into two pieces and then recombined to withstand stretching. One sample was dyed with methyl red.

Recycled 1   **Recycled 2**   **Recycled 3**   **Recycled 4**
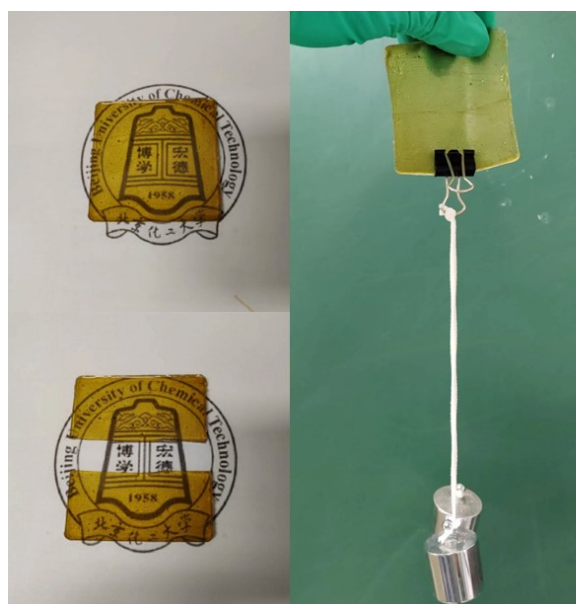

Fig. S29. Optical images of THICE after 4 cycles, and the healed sample (0.2 cm (T) × 6 cm (W) × 5 cm (L)) withstood a 200-g load after the 4th cycle.

Table S2 The mechanical properties and conductivity of recycled THICE.

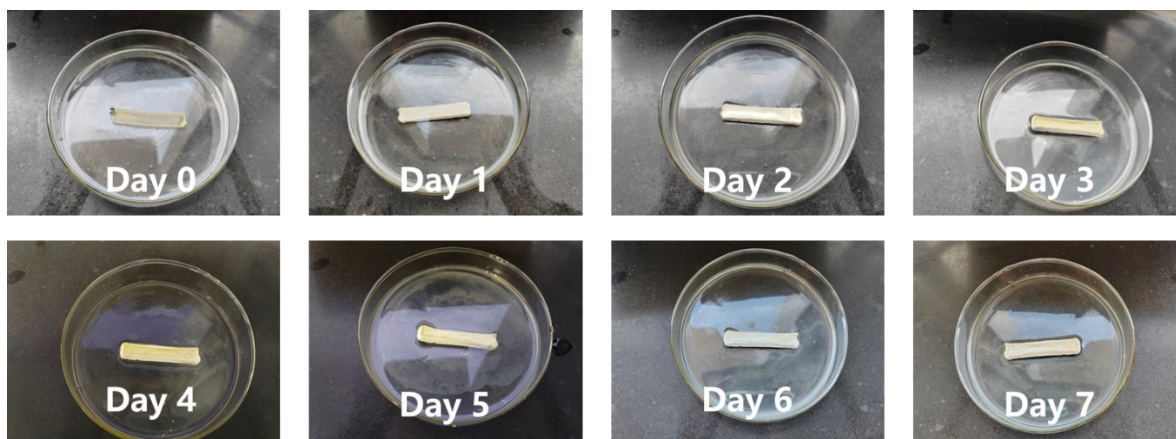|	Elongation at break (%)	Tensile strength (MPa)	Conductivity $10^4\sigma$ (S·m⁻¹)
Original	473 ± 34	0.47 ± 0.04	4.09 ± 0.58
1st	457 ± 12	0.47 ± 0.02	3.21 ± 0.49
2nd	430 ± 19	0.46 ± 0.02	2.92 ± 0.86
3rd	425 ± 12	0.45 ± 0.03	2.23 ± 0.86
4th	362 ± 14	0.39 ± 0.01	1.56 ± 0.72

Figure S30 Digital pictures of the THICE immersed in the H$_2$O for 7 days.
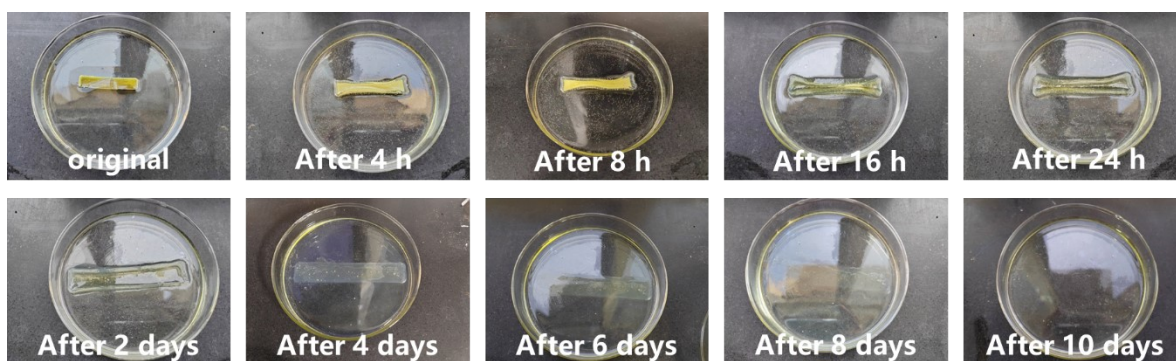

Figure S31 Digital pictures of the THICE immersed in a 1 mol·L^{-1} NaHCO$_3$ aqueous solution
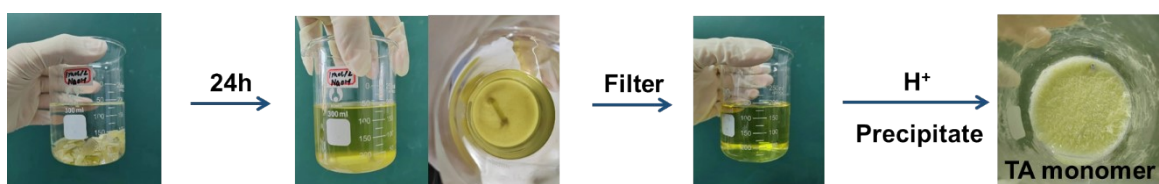
for 10 days.

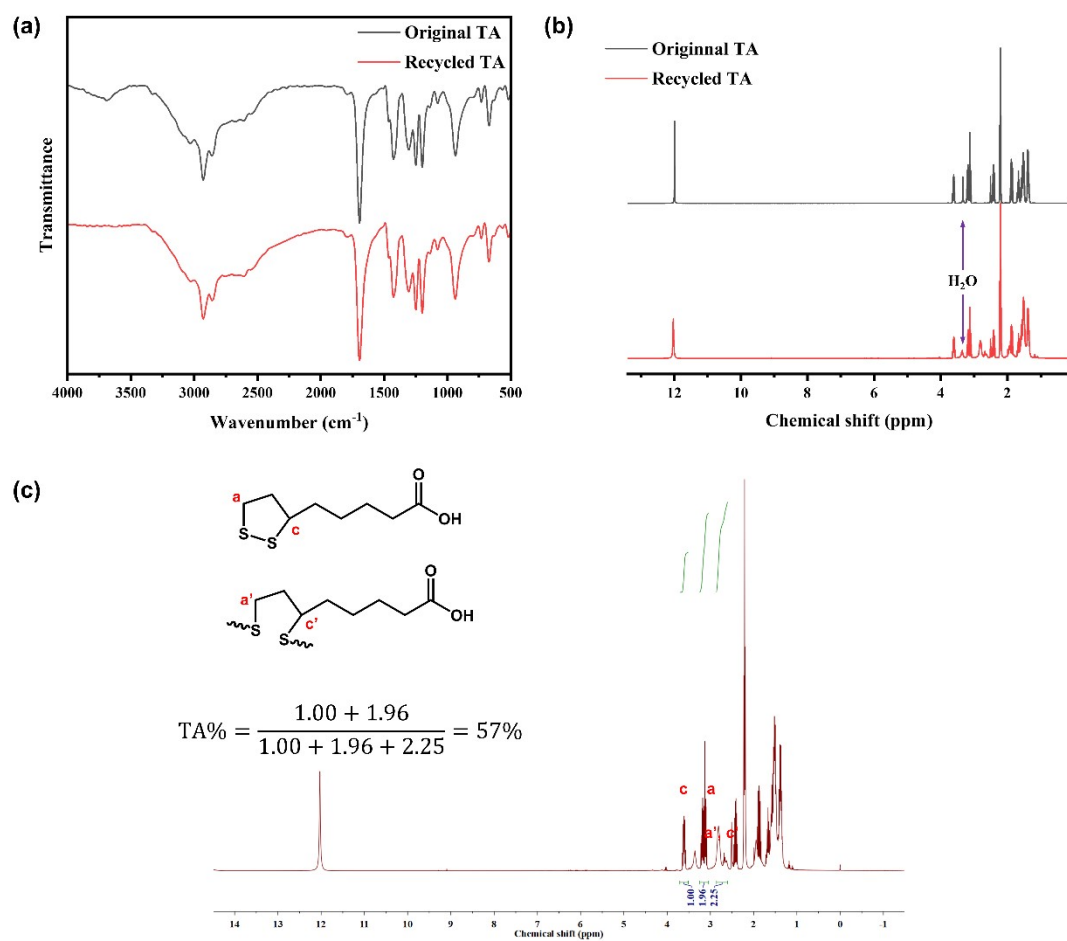**Figure S32** Recover TA monomer formed by hydrolysis and acidification.

Figure S33 (a) FT-IR spectra and (b) ^{1}H NMR spectra of original and the recycled TA

monomers; (c) calculation of TA and oligomeric polyTA content in recycled products.

Table S3 The comparison between this work and prior publish results.

Ref.	materials	Max. strain (%)	Max. stress	Self-healing	Transparency	Ionic conductivity (S m^{-1}) at R.T.	Recyclability	green feedstocks
55	TA/ Acrylic acid/ cellulose Ionic gel	1250	0. 8 MPa	1h, 100℃, 92.2%	84.7%	7.4×10^{-3}	√	√
56	TA/itaconic acid Ionic gel	800	187.2 kPa	15h, 90.1%	>90%	0.37×10^{-2}	√	√
60	TA/LiTFSI	1585%	224.9 kPa	3h, 90.3%	86.7%	2.14×10^{-5}	√	√
61	TA/DMA/LiTFSI	1150%	≈97 kPa	78-118%	None	1.4×10^{-6}–2.7×10^{-5}	None	√
31	2-methoxyethyl acrylate	1420%	0.52 MPa	\	>80%	5.4×10^{-5}	None	None
32	Acrylic acid Ionic gel	1300%	0.4 Mpa	48h, 91.5%	93.1%	7.8×10^{-2}	None	None
33	Acrylic acid Ionic gel	450%	0.6 MPa	72 h, 94%	95%	4.0×10^{-2}	None	None
70	Acrylic acid / Cellulose Nanofiber Ionic gel	290%	0.8 MPa	\	90%	1.8×10^{-1}	None	None
71	PEO	563%	0.9 MPa	84h, 96%	78%	2.04×10^{-2}	None	None
This work	**TA/HA**	**3000**	**1.15 Mpa**	**16 h, 82%**	**94%**	**4.49×10^{-4}**	**√**	**√**